

A comparative study of granular activated carbon and sand as water filtration media with estimation of model parameters

Jaideep Chatterjee*, Shajahan A, Shailendra Pratap and Santosh Kumar Gupta

Unilever R&D, Bangalore Laboratory, 64 Main Road, Whitefield, 560066, Bangalore, India

(Received January 20, 2017, Revised April 24, 2017, Accepted April 25, 2017)

Abstract. The use of Granular Activated Carbon (GAC) and naturally occurring silica (Sand) as filtration media in water and waste water treatment systems is very common. While GAC offers the additional functionality of being an “adsorptive” filter for dissolved organics it is also more expensive. In this paper we present an experimental evaluation of the performance of a bed of GAC for colloid removal and compare the same with that from an equivalent bed of Sand. The experiments are performed in an “intermittent” manner over extended time, to “simulate” performance over the life of the filter bed. The experiments were continued till a significant drop in water flow rate through the bed was observed. A novel “deposition” and “detachment” rate based transient mathematical model is developed. It is observed that the data from the experiments can be explained by the above model, for different aqueous phase electrolyte concentrations. The model “parameters”, namely the “deposition” and “detachment” rates are evaluated for the 2 filter media studied. The model suggests that the significantly better performance of GAC in colloid filtration is probably due to significantly lower detachment of colloids from the same. While the “deposition” rates are higher for GAC, the “detachment” rates are significantly lower, which makes GAC more effective than sand for colloid removal by over an order of magnitude.

Keywords: water purification; activated carbon; empirical model; filtration; transient model

1. Introduction

The use of granular activated carbon (GAC) is common in the purification of water. These materials are typically derived from coconut shells or palm shells (Mohammed *et al.* (2015)) or even uncommon materials like pomegranate peel (Rouabeh and Amrani (2012)). In addition to being a natural adsorptive material for many organic pollutants, GAC is also an excellent media for the removal of fine colloids. However, during use, GAC filters (Chatterjee and Gupta (2014)), columns and beds, can get clogged due to the deposition of colloidal matter on its surface. The phenomena of clogging of granular beds or columns with age is similar in systems as diverse as large sand based filtration plants to small powdered activated carbon based home use potable water filters. The mechanisms of sediment deposition and the resultant reduction of water flow due to clogging is similar across the above processes. This phenomenon may also be observed when

*Corresponding author, Ph.D., E-mail: jaideep.chatterjee@unilever.com

ionic contaminants are removed from water (Hamid and Lee (2016), Kalpaklı (2015)) using solid materials and media in large scale systems. In this paper we report an experimental study and a mathematical model, which looks at the deposition of natural inorganic colloids in columns consisting of different filtration media. The decline in the bed porosity over time and space and the resultant water flow rate decline are modeled for these different media. The model is developed using the “deposition-rate” based approach to modeling the process of colloid deposition during flow through saturated porous media. Flow of water through saturated porous media, which is of interest in contaminant transport in groundwater, has also received a lot of attention recently (Ahmadi *et al.* (2016), Satavalekar and Sawant (2015)), although they deal with transport of soluble contaminants as compared to the transport of colloids, which is discussed in this paper.

Many studies on the variation of colloid deposition with media age have been performed, in the context of water filtration. These studies were performed at constant water flow-rate, wherein the pressure-drop across the medium increased due to deposition of colloids (Darby and Lawler (1992), Tobiasson and Vigneswaran (1994), Vigneswaran and Tulachan (1998)). These conditions are different from the gravity driven water flow through depth filters and filter beds. If constant flow is maintained through filter beds, the media fails to remove colloids after some time. This can be attributed to detachment of deposits (Bai and Tien (1997)) as colloid-deposits build-up, the reduction of deposition due to an increase in the interstitial velocity and to the “blocking” of deposition sites by previous deposits. Unlike the above systems, gravity driven filters and filter beds fail when the flow rate of water becomes too low. This study mimics the “life-span” of gravity driven depth filters which fail due to clogging.

The colloid-removal variation with media age, under constant flow conditions, has been modeled extending the microscopic trajectory-analysis approach used in filtration developed by Rajagopalan and Tien (1977), Tien and Ramarao (2007). In these models, the single-collector-efficiency of a media grain, which is depth-invariant, is varied with age, by assuming that the deposited colloids initially act as additional collectors, thereby increasing the overall single collector efficiency. With time, the deposited colloids contribute to head-loss, which causes the interstitial velocity to increase, eventually leading to a reduction of deposition. These models need several parameters to quantify the above effect and have been shown to match the reduction in removal performance with age of the media. A transient model for a depth filter over its entire life can be found in (Gitis *et al.* (2010)), which uses 3 different time-dependent deposition-rates. It has also been shown that the distance-wise variation in colloid-concentration in the aqueous-phase can be simulated by material-balance based models using the kinetic parameter termed deposition-rate, k , which can be related to the parameters used in trajectory analysis. The use of the material-balance based equations for simulating the transient performance of saturated-porous-media columns have also been reported (Tufenkji (2007)). It has been shown that the use of dual and multiple-deposition-rates, k_i , can lead to improved estimation of colloid reduction during water transport through “clean” saturated-porous-media columns (Tufenkji *et al.* (2003), Tufenkji and Elimelech (2004), Tufenkji and Elimelech (2005a), Tufenkji and Elimelech (2005b), Foppen *et al.* (2007), Li *et al.* (2004)). The above has led to an increased use of “deposition-rates”, as compared to the microscopic trajectory analysis parameters, for modeling colloid deposition in saturated porous media.

In this paper, we report an experimental study using sand and activated carbon as porous media, wherein the variation in the liquid-phase colloid-concentration over distance, $C(x)$, is measured under intermittent flow driven by hydrostatic head. The $C(x)$ data show significant changes with age. In order to test if the simulation of the above data requires the use of time

dependent deposition-rates, we develop a material-balance based transient model. This model is based on depth and time-invariant deposition-rates. It accounts for “blocking” of deposition by previously deposited colloids and as well as detachment of deposited colloids. It is observed that the model is capable of simulating the “clean” porous-media $C(x)$ variation, as well as the variation of $C(x)$ with media-age. The model is also capable of explaining the variation of the solid-phase-deposit density, $S(x)$, and the pore velocity and porosity variation with depth and age. In addition this model is applicable to different media, namely sand and activated carbon, which demonstrates the generic nature of the model and its applicability to a wide range of materials.

2. Model for transient variation in colloid deposition

Colloid filtration theory predicts a log-linear variation of $C(x)$ with transport distance, x , assuming a homogeneous colloid population (Rajagopalan and Tien (1977)). However many studies have reported deviation from log-linearity in $C(x)$ curves for several colloidal systems (Tong *et al.* (2005), Brown and Abramson (2006), Tong and Johnson (2007), Chatterjee and Shajahan (2010)). While the above has been attributed to several phenomena such as sieving (Bradford *et al.* (2003), Bradford *et al.* (2005), Bradford and Bettahar (2006), Bradford *et al.* (2007)), it has also been shown that material balance and deposition-rate based models with two or more deposition-rates can simulate the above deviation of $C(x)$ from log-linearity (Tufenkji and Elimelech (2005b), Chatterjee and Gupta (2009), Chatterjee *et al.* (2011)). It may be noted that “sieving” is mathematically identical to having a higher deposition rate near the top of the porous media column.

If the colloidal population is considered to consist of population segments such that each population segment has a distinct deposition-rate, then unsteady-state material balance of colloids of type m , over a small section of the media leads to

$$-u \frac{\partial c_m}{\partial x} + \varepsilon D_m \frac{\partial^2 c_m}{\partial x^2} = \rho_b \frac{\partial S_m}{\partial t} + \frac{\partial (\varepsilon c_m)}{\partial t} \quad (1)$$

Where $c_m(x,t)$ is the liquid-phase concentration of colloid type m at distance x and time t , in mg/cm^3 , $S_m(x,t)$ is the solid-phase deposit density of the colloid type m at distance x and time t , in $\text{mg colloids}/\text{gm medium}$, $u(t)$ is the superficial velocity at time t , in cm/sec , ρ_b is the bulk density of the medium in gm/cm^3 , D_m is the hydrodynamic dispersion coefficient in cm^2/sec and $\varepsilon(x,t)$ is the porosity of the medium at distance x and time t . The flux due to hydrodynamic dispersion of colloidal particles is neglected since it is expected to be insignificant for the colloids and flow velocities of interest in this study. It may be noted that while pore velocity, v , is expected to vary with distance and time, the superficial velocity u , is distance invariant. Hence its distance-derivative is omitted in the first term of Eq. (1). These simplifications lead to

$$-v \frac{\partial c_m}{\partial x} = \frac{\rho_b}{\varepsilon} \frac{\partial S_m}{\partial t} + \frac{\partial c_m}{\partial t} + \frac{c_m}{\varepsilon} \frac{\partial \varepsilon}{\partial t} \quad (2)$$

Where $v(x,t)$ is the fluid pore velocity at distance x and time t , in cm/sec . The rate of deposit build-up on the media is assumed to be proportional to the local liquid-phase colloid-concentration. However with age, deposition is diminished due to blocking of media surface by previous deposits as well as due to colloid detachment from the media, (Bai and Tien (1997),

Bergendahl and Grasso (2000)) the rates of both of which can be expected to be proportional to the solid-phase-deposit-density. If d_m is considered to be the rate-constant for detachment and b_m the rate-constant for blocking, for colloid-type “ m ”, then the following kinetic equation can be used to express the rate of increase of deposits

$$\frac{\rho_b}{\varepsilon} \frac{\partial S_m}{\partial t} = k_m c_m - \rho_b d_m S_m - \rho_b b_m S_m \quad (3)$$

Where k_m is the deposition-rate of colloid type m having units of 1/time, d_m and b_m are as defined above also having units of 1/time. Eqs. (1)-(3) are subject to the following boundary and initial conditions: $c_m(0,t)=c_{m,0}$, $v(x,0)=v_0$, $\varepsilon(x,0)=\varepsilon_0$, $S(x,0)=0$.

In the above, the deposition, detachment and blocking-rates for a colloid type are distance and time-invariant in contrast to some previously reported models which used a “filter-coefficient”, that is dependent on the local solid-phase deposit density. Combining the material balance Eq. (2) and the kinetic Eq. (3) we get

$$-\frac{\partial c_m}{\partial x} = \frac{1}{v} \frac{\partial c_m}{\partial t} + \frac{c_m}{\varepsilon v} \frac{\partial \varepsilon}{\partial t} + \frac{k_m}{v} c_m - \frac{\rho_b l_m}{v} S_m \quad (4)$$

and

$$\frac{\partial S_m}{\partial t} = \frac{\varepsilon k_m}{\rho_b} c_m - \varepsilon l_m S_m \quad (5)$$

Where $l_m=d_m+b_m$, and the other terms have been defined earlier. The above system of equations can be solved by a finite-difference method, to simulate the variation of $c(x,t)$, $S(x,t)$, $\varepsilon(x,t)$ and $v(x,t)$. The equations for $\varepsilon(x,t)$ and $v(x,t)$ are discussed later. The computational procedure used is as follows. First the “clean” porous-media-column flow-rate was estimated, with the experimentally determined media porosity, hydrostatic head, length of the porous-medium and other experimental parameters (shown in Table 1). It is known that the superficial velocity, for laminar flow through a packed column can be obtained by Eq. (6),

$$u = \frac{\Delta P}{(25/6) \mu L} \frac{\varepsilon_0^3}{(1-\varepsilon_0)^2} \frac{1}{a_v^2} \quad (6)$$

Where ΔP is the driving pressure, μ is the water viscosity, L is the length of the porous-media-column, ε_0 is the initial porosity of the “clean” column and a_v is the surface area per unit volume of the media. The computed flow-rate matched the observed flow-rate, when the ratio of a_v for the medium and the a_v for spheres is as shown in Table 1. The “clean” porous-media-column $C(x)$ data suggest that there are only 2 population segments thereby restricting m to 2. Next the values of k_1 and k_2 , the depth and time invariant deposition-rates for the two population segments, were estimated from the clean-media $C(x)$ data. The values of f_1 and f_2 , the fractions of the fast and slow depositing colloids, in the input colloidal population, were also obtained from the above. These values are shown in Table 2. The finite difference form of Eq. (4) was then used to estimate the liquid-phase colloid-concentration of colloid-type m , for the clean-porous-media-column. The total liquid-phase colloid-concentration, at a point in space and time, can be estimated as

$$C(i, j) = \sum_m C_m(i, j) \quad (7)$$

Table 1 Summary of the experimental conditions

	Sand	Activated Carbon
Excess Hydrostatic head, cm	11	11
Column Height, cm	45	45
Mass of media, gm	450	130
Column ID, cm	3.1	3.1
Mean Media grain size, μm	350	400
Fluid Viscosity, g/cm.s	0.01	0.01
ε_0 Initial column porosity	0.48	0.40
Colloid density, g/cm ³	2.65	2.65
ε_d Porosity of deposits	0.7	0.5
a_v Media/ a_v spheres	1.85	1.4

Where “ i ” represents the spatial-section-number and “ j ” represents the time interval. The solid-phase deposit density $S(x)$ is 0 for all sections of the clean-porous-media-column. The solid-phase deposit-density of colloids of type m , $S_m(i,j)$, at the end of the first time interval was estimated by using a finite-difference form of Eq. (5). The total deposit density on the media in any section, i , at time, j , can be estimated from

$$S(i, j) = \sum_m S_m(i, j) \quad (8)$$

These values of $S(i,j)$ were used to estimate the porosity of each section after the first time interval using Eq. (9). The porosity of the i^{th} section in the j^{th} interval can be expressed as

$$\varepsilon(i, j) = \varepsilon(i, 0) - \left(\frac{\rho_b 10^{-3}}{\rho_c (1 - \varepsilon_d)} \right) S(i, j) \quad (9)$$

Where ρ_c is the true density of the colloidal particles and ε_d is the porosity of the deposited colloidal layer and the factor 10^{-3} is required since S is in mg/g and ρ_c is in g/cm³. If Eq. (6) is applied to estimate the pressure drop across the i^{th} section in the j^{th} interval, we get

$$\Delta P(i, j) = u(i, j) \frac{25}{6} \mu \Delta x \frac{(1 - \varepsilon(i, j))^2}{\varepsilon(i, j)^3} a_v^2 \quad (10)$$

Recognizing that superficial velocity in the j^{th} interval would be the same for all the sections, if we now add up the individual section pressure drops to get the overall pressure drop, which on re-arrangement gives

$$u(j) = \frac{\Delta P}{\frac{25}{6} \mu \Delta x a_v^2 \sum_i \frac{(1 - \varepsilon(i, j))^2}{\varepsilon(i, j)^3}} \quad (11)$$

The superficial velocity for the next time interval was estimated using Eq. (11). From the new superficial velocity and the porosities of each section from the same time interval, the new interstitial velocities were estimated for each section by

$$v(i, j) = \frac{u(j)}{\varepsilon(i, j)} \quad (12)$$

Finally the flow-rate for time interval j , $Q(j)$, was estimated by

$$Q(j) = A u(j) \quad (13)$$

where A is the cross sectional area of the porous-media-column. The above sequence was repeated for subsequent intervals. In the experiments, $C(x)$ values were recorded after fixed volume intervals. Hence in the simulation volume increment was also fixed, instead of the time increment, which caused the incremental time to increase gradually as the flow-rate declined. In the following sections the experiments performed and the resulting data are described. We then discuss the ability of the above model to explain the observations across different types of filtration media.

3. Materials and methods

3.1 Porous media columns

75 cm long borosilicate glass column, with internal diameter of 3.1 cm, with spaced sampling ports was fabricated and calibrated for height and volume. The column was filled with 450 gm of irregular silica particles (sand) in the size range of 300-350 μm . The chemical composition of quartz sand was 99.89% SiO_2 , 0.02% Al_2O_3 , 0.01% Na_2O and 0.001% Fe_2O_3 . The material was sourced from Master Micron, Bangalore, India. Prior to use, the sand was rinsed with de-ionized water (DI), till the rinse water did not show any change in pH and conductivity. The porous-media-column was prepared by partially filling the column with DI water and gradually adding known amounts of cleaned and dried sand from the top. The sand grains were allowed to settle under gravity. The increase in the water level and the apparent height of the sand column were noted. This gave the estimated porosity of the filter media which was 0.48. The path length of the filter-media column was 45 cm.

Similar method was used to prepare filtration media columns of activated carbon. Acid washed activated carbon, from Active Carbon, Hyderabad, India was used in this study. The size range of the activated carbon was 300-500 μm . The carbon granules were washed repeatedly with DI water, till the wash water did not show any change in pH. The carbon granules were then dried. Following this the granules were soaked in a known volume of water for sufficient time to allow the water to penetrate the pores of the granules. After this the slurry was gently stirred to remove any air bubbles. The slurry was then filled into a 75 cm column containing a fixed quantity of DI water. The water level increase was noted. Since the volume of water in the slurry was known, the true volume of the carbon granules was estimated. The apparent volume of the activated carbon bed was also noted. This gave the bed porosity, which was 0.4. The above method is required as the dried activated carbon granules do not settle to form a bed. Dry carbon granules are buoyed up by the air contained in the pores. The media was kept submerged in water throughout the experiments. The aqueous-phase in contact with the media in the column did not show any change in pH over days.

3.2 Colloidal particles

The colloids used in this study consisted of inorganic dust obtained from Powder Technology

Inc., MN, USA. Chemical composition of this material was reported to be 68-76% SiO₂, 10-15% Al₂O₃, 2-4% Na₂O, 2-5% K₂O, 2-5% Fe₂O₃, 2-5% CaO, 1-2% MgO and 0.5-1% TiO₂. Particle size analysis of this colloid in DI water showed that 10% of the population by volume was below 1.16 μm, 50% of the population was below 2.34 μm and 90% was below 4.93 μm. The density of the colloidal particles was 2.65 gm/cm³. The particles were irregular in shape.

3.3 Water chemistry

The liquid-phase used in the study was Milli-Q water whose composition was varied by adding NaCl, (≥99.5% pure) or CaCl₂·2H₂O, reagent grade, obtained from Merck. The reasons behind the choice of the levels of electrolytes are discussed in the last section. 100 mg/L of inorganic dust was added to the aqueous-phase after the addition of the electrolytes. Small pH adjustment was required to obtain an aqueous-phase pH of 6.9±0.2, which was constant throughout the experiments. The aqueous-phase thus prepared was gently stirred over the duration of the experiments.

3.4 Porous-media-aging experiments

The column was preconditioned by passing the aqueous-phase without the colloids. The input aqueous-phase was pumped to the top of the porous-media-column, to maintain a constant hydrostatic head of 11±0.5 cm above the media. The initial flow-rate was 50 ml/min which declined during the course of the experiment. This flow-rate corresponds to a superficial velocity of ~4 m/hr. Flow was stopped after 10 L of aqueous-phase had been passed. The porous-media-columns were maintained in the submerged state overnight. Next day, flow was restarted through the column and another 10 L was passed. This was continued till the end of the experiment. The experiments reported here were run for up to 20 days in the above semi-continuous mode, during which the effluent concentration was measured. At regular intervals samples were drawn from the side ports, in such a way that the samples were collected at almost the same time. These samples are analyzed for mass concentration by turbidity measurement, using a turbidity meter, "Turbiquant" from Merck, which was calibrated with 0.02, 10 and 1000 NTU standards prior to use.

3.5 C(x) measurements

Estimation of the mass concentration of the colloids in the liquid-phase was performed in the following manner. Calibration curves were generated by adding different levels of inorganic dust ranging from 0 to 300 mg/L and measuring the resultant turbidity. The calibration data were best represented by a quadratic fit, which resulted in R² value in excess of 0.998. If the turbidity value fell below 10 NTU, a calibration based on a linear fit, which resulted in R² value in excess of 0.999, was used. In the experiments the turbidity was measured and the resulting mass concentration was estimated from the calibration curves. The mass densities obtained from turbidity measurements were occasionally verified by gravimetric techniques.

3.6 S(x) measurements

Estimation of the solid-phase deposit density $S(x)$ was performed in the following manner. At

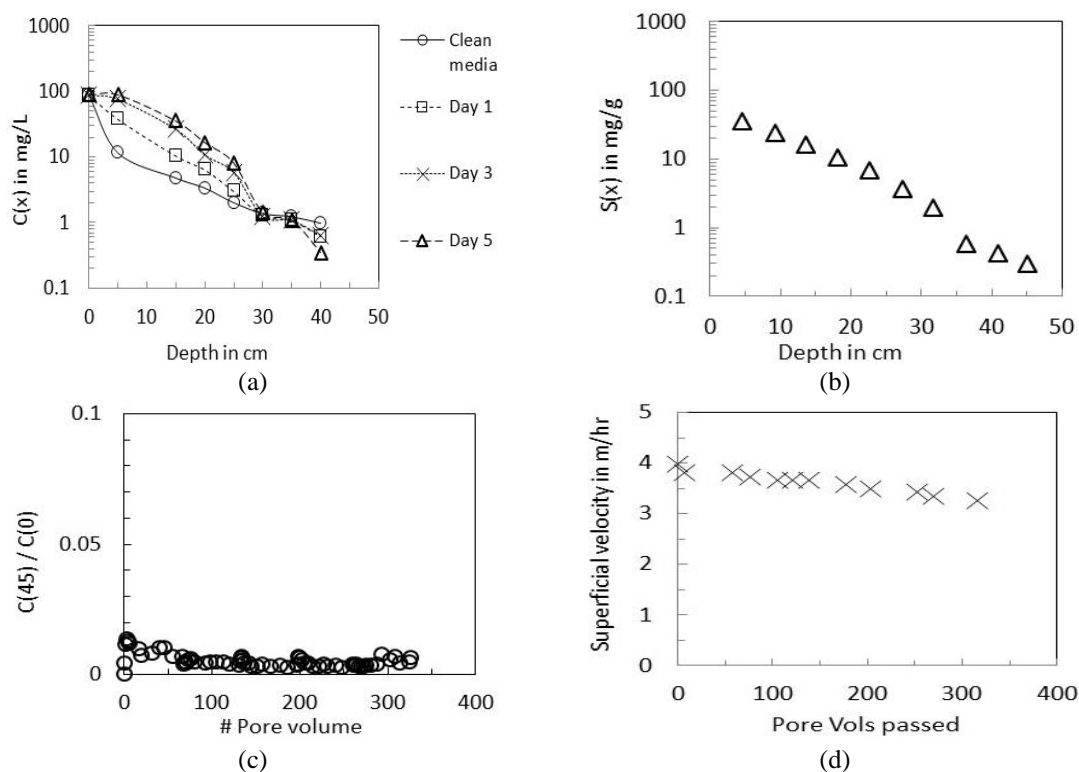


Fig. 1(a) The measured variation of $C(x)$ versus x obtained from the “clean” sand column and from the same over 5 (50 L) days. (b) The measured variation of the deposit density in mg of colloids/gm of media, $S(x)$, versus x obtained from the sand column after the 5th day. (c) The measured normalized effluent concentration. (d) The measured variation in the superficial velocity with volume of water passed

the end of the experiment, which varied from 5 days to 20 days, the saturated-porous-media column was drained. Media was extracted from different depths of the column. These small samples of the media were washed in measured quantities of Milli-Q water. The eluted deposits were dispersed in the aqueous phase. The turbidity of these wash-water samples was measured, from which the mass density of the colloids in the aqueous-phase were estimated. This required the use of a new calibration curve relevant for high colloid-concentrations and their turbidities. From these mass-densities, the absolute amount of eluted colloids in the media samples was estimated, which was divided by the mass of the cleaned dried media samples to obtain $S(x)$. To verify the validity of using turbidity measurements for estimating colloid density in the wash water samples, the particle size distribution of the eluted colloids was measured. This was found to be very similar to that of the colloids in the input aqueous-phase.

4. Results

The experimental observations are reported in Figs. 1-3. The first experimental system consisted of a sand column, an aqueous suspension of the colloids (100 mg/L), where the aqueous

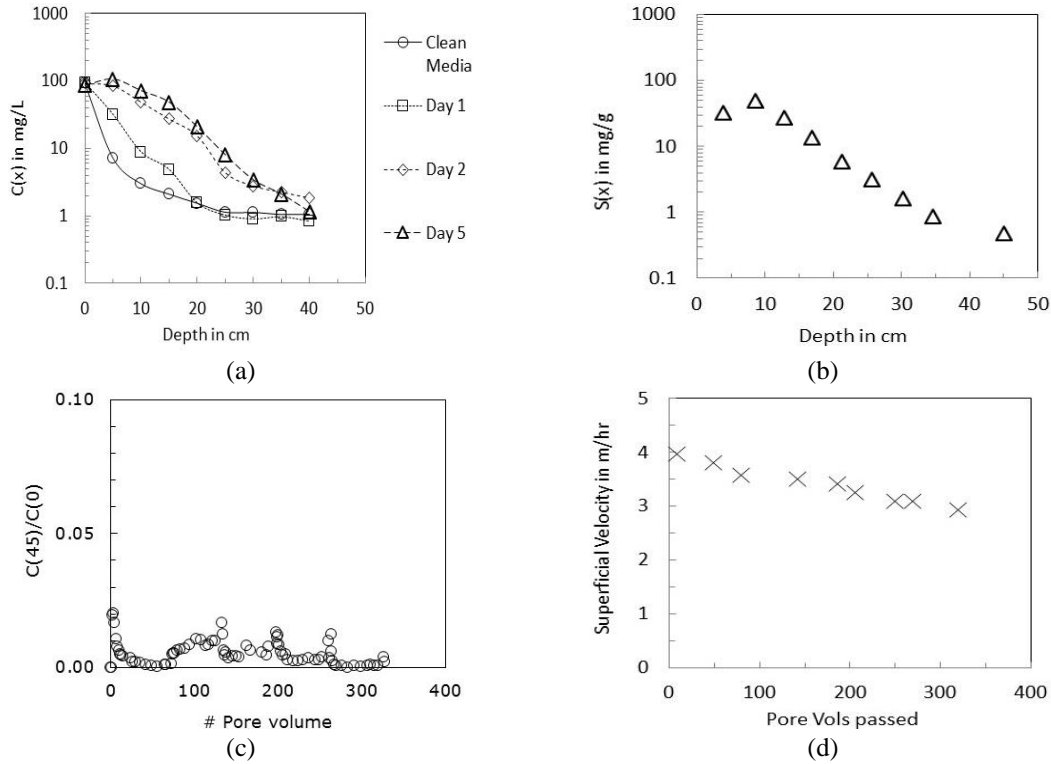


Fig. 2(a) The measured variation of $C(x)$ versus x obtained from the clean sand column and from the same over 5 days. (b) The measured variation of the solid-phase-deposit-density expressed in mg of colloids/gm of media, $S(x)$ versus x obtained from the sand column after the 5th day. (c) The measured normalized effluent concentration. (d) The measured variation in the superficial velocity with volume of water passed

phase contained 200 mM NaCl. The $C(x)$ data are shown in Fig. 1(a). The lines have been provided to improve readability, and do not represent the model. After 50 L of the aqueous-suspension had been passed through the column, the media was extracted from the column and the colloid-deposit-density was estimated based on the procedure described in the previous section. These data are shown in Fig. 1(b). The normalized effluent-colloid concentration remains very low with 99% colloid removal in the column over the duration of the experiment. The normalized effluent-colloid-concentration data are shown in Fig. 1(c). The measured variation in the superficial velocity (at constant head) over the duration of the experiment is shown in Fig. 1(d).

For the second experiment, the media was identical to the first, and only the electrolyte and its concentration was varied. The electrolyte used was CaCl_2 and its concentration was 3 mM. The log $C(x)$ versus x data from the aging column and the solid-phase deposit-density data from this experimental system are shown in Figs. 2(a) and 2(b). The lines have been provided to improve readability, and do not represent the model. The effluent-colloid-concentration data and the superficial velocity decline data are shown in Figs. 2(c) and 2(d). While we report data from two experiments, these experiments were repeated several times. The data reported above are consistent with the observations from several repetitions.

The third experiment was conducted with media column consisting of activated carbon, and an

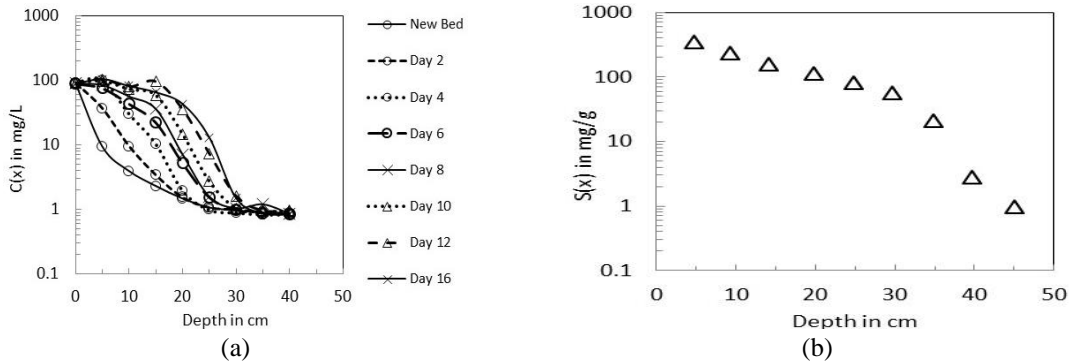


Fig. 3(a) The measured variation of $C(x)$ versus x obtained from the clean activated carbon column and from the same over 19 days. (b) The measured variation of the solid-phase-deposit-density expressed in mg of colloids/gm of media, $S(x)$ versus x obtained from the activated carbon column after the 19th day

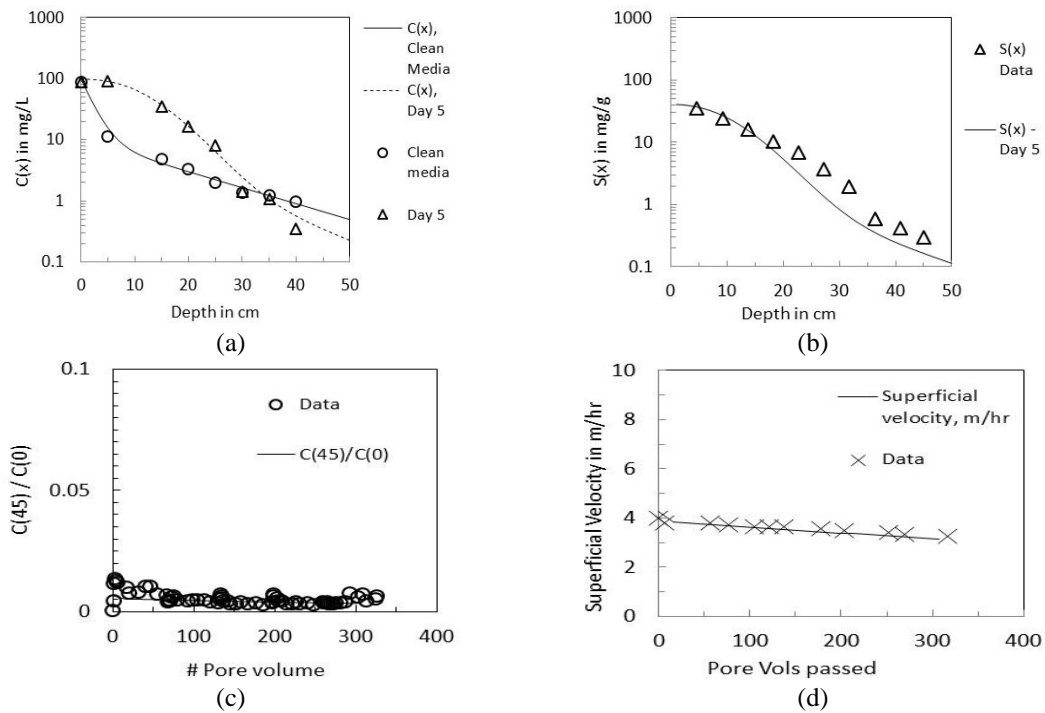


Fig. 4(a) Computed and measured variation of $C(x)$ versus x , for the experimental conditions shown in Fig. 1. $C(x)$ values are shown for the “clean” sand column and the same, after Day 5. (b) The computed and measured variation of $S(x)$ versus x obtained from the sand column after Day 5. (c) The computed and measured variation of the normalized effluent concentration with number of pore volumes (d) The computed and measured variation in superficial velocity with pore volumes, for the experimental conditions shown in Fig. 1

aqueous phase containing the above colloid concentration with 3 mM CaCl_2 as the electrolyte. Due to the significantly higher capacity of activated carbon for colloid removal, this experiment lasted

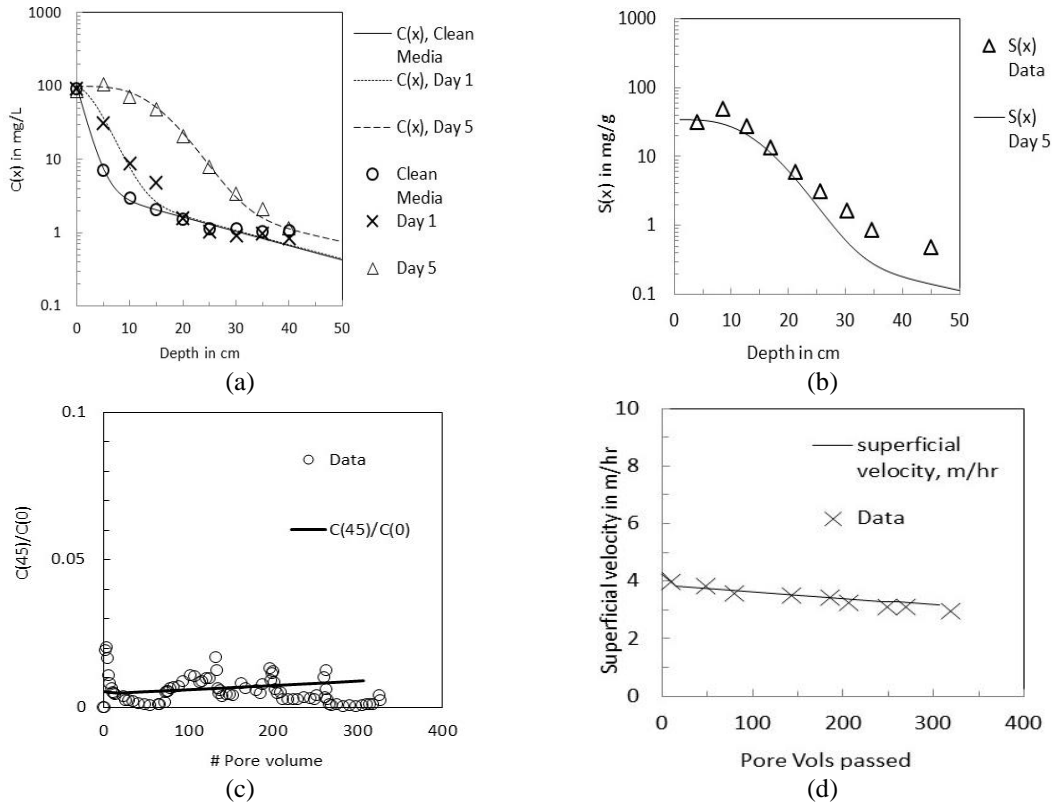


Fig. 5(a) Computed and measured variation of $C(x)$ versus x , for the experimental conditions shown in Fig. 2. $C(x)$ values are shown for the “clean” sand column and for the same, after Day 1 (10 L) and Day 5 (50 L). (b) The computed and measured variation of $S(x)$ versus x obtained from the sand column after day 5 (c) The computed and measured variation of the normalized effluent concentration with number of pore volumes (d) The computed and measured variation in superficial velocity with pore volumes, for the experimental conditions shown in Fig. 2

Table 2 Values of the model parameters which were used to obtain the model predictions shown in Figs. 4 to 9

	Sand with 200 mM NaCl	Sand with 3 mM CaCl ₂	Activated Carbon with 3 mM CaCl ₂
f_1 (fast)	0.9	0.96	0.96
f_2 (slow)	0.1	0.04	0.04
K_1 (1/sec)	0.15	0.21	0.21
K_2 (1/sec)	0.015	0.011	0.011
L_1 (1/sec)	0.00027	0.00045	0.00018
L_2 (1/sec)	1×10^{-7}	2×10^{-5}	5×10^{-6}

over 19 days, before a level of media saturation was reached which necessitated stopping the experiment. In contrast, the experiments with sand as the media lasted only ~5 days. The log $C(x)$ versus x data from the aging column and the solid-phase deposit-density data from this experimental system are shown in Figs. 3(a) and 3(b). The lines have been provided to improve

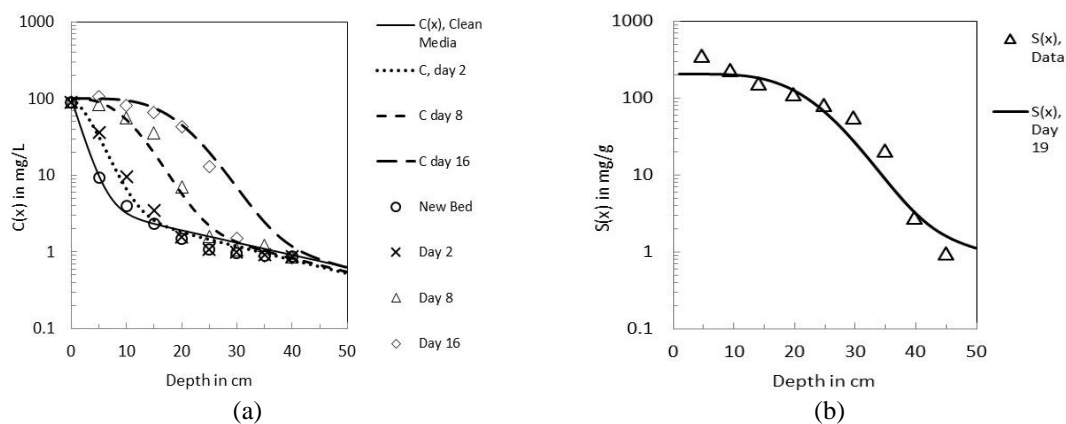


Fig. 6(a) Computed and measured variation of $C(x)$ versus x , for the experimental conditions shown in Fig. 3. Computed variations of $C(x)$ are shown for the “clean” activated carbon column and for the same, after day 2, day 8 and day 16. (b) Computed and measured variation of $S(x)$ versus x obtained from the activated carbon column after day 19, for the experimental conditions shown in Fig. 3

readability, and do not represent the model.

Figs. 4 and 5 show the computed variations of (a) $C(x)$, (b) $S(x)$ with distance, x , and the measured values of the same, over the duration of the experiments, for the experimental conditions reported in Fig. 1 (experiment 1) and Fig. 2 (experiment 2) respectively. The computed and measured variations of the (c) effluent-concentration and (d) superficial velocity, u , with number of pore volumes passed, are also shown.

The computed curves in Fig. 4 were obtained using model parameters shown in the column 1 of Table 2. The computed curves of Fig. 5 were obtained using parameters shown in column 2 of Table 2.

Fig. 6 show the computed variations of (a) $C(x)$, (b) $S(x)$ with distance, x , and the measured values of the same, over the duration of the experiments, for the experimental conditions reported in Fig. 3 (experiment 3). The computed curves shown in Fig. 6 were estimated using parameter values which are reported in column 3 in Table 2.

To obtain the “clean” column $C(x)$ estimates, the parameters required are the 2 deposition-rates k_1 and k_2 and the fractions of the fast and slow depositing colloids, f_1 and f_2 . The additional parameters for the transient model are the 2 deposit-loss rates l_1 and l_2 which combine the deposit-loss due to blocking and the loss of deposits due to detachment. The only additional parameter required for estimating the flow-rate decline is the porosity of the deposits ε_d . The value of this porosity used in the calculations was 0.7 for the sand and 0.5 for the activated carbon. This can be due to the “open” structure that arises from the random build-up of particles of a narrow size distribution. This parameter value is similar to a value of 0.8 reported when the sand grains are saturated with deposits. This value has not been reported for activated carbon media. The estimation of $S(x)$ does not require any additional parameters.

5. Discussion

In this section, first, the points of similarity between the 3 experimental systems, involving the

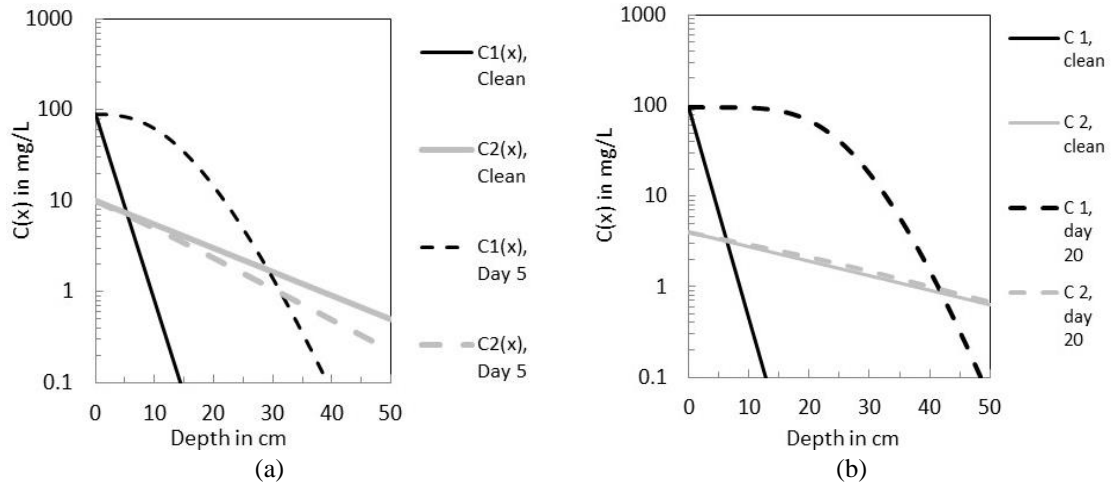


Fig. 7 Computed variation in the concentration of the two distinct population segments, $C_1(x)$ and $C_2(x)$ with depth, for (a) the sand column using parameters shown under the column 1 in Table 2 (b) for the activated carbon column using parameters shown under column 3 in Table 2

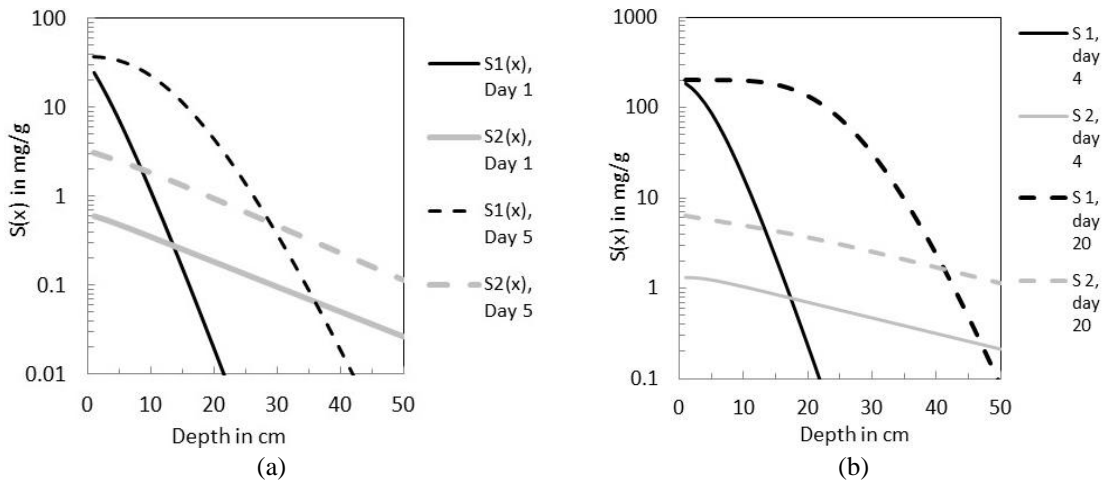


Fig. 8 Computed variation in the solid-phase deposit density of the two distinct population segments, $S_1(x)$ and $S_2(x)$ with depth, for (a) the sand column using parameters shown under the column 1 in Table 2 (b) for the activated carbon column using parameters shown under column 3 in Table 2

two types of media, the two electrolytes and their concentrations, are discussed. This is mainly based on the observation that all 3 diverse experimental systems can be described well by the same model, which has been described in detail in section 2. In the second part of this section the differences between the experimental systems, with special emphasis on the differences between Activated Carbon and Sand as the water filtration media is discussed. The effect of the electrolytes and their concentrations are also discussed in this section.

Figs. 1 to 3 show that when the porous-media is “clean”, the slope of the measured $C(x)$ curve in the section at the top is high, and a point-of-inflection is observed down-stream of which the slope of the $C(x)$ curve is low. This is observed for both the sand and the activated carbon media.

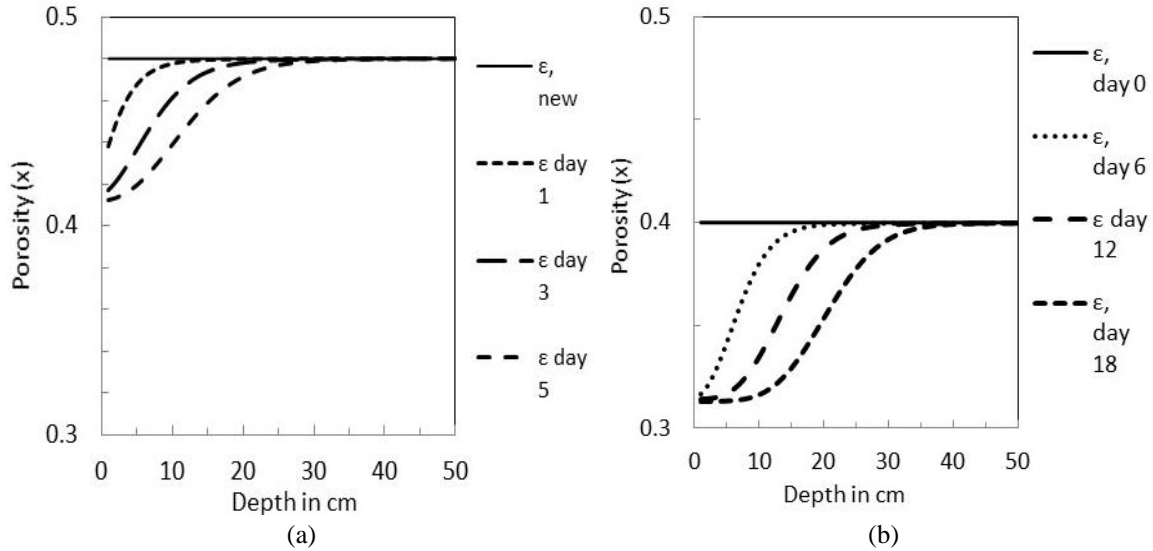


Fig. 9 Computed variation in the porosity of the column with depth, $\varepsilon(x)$, with age for (a) the sand column (b) for the activated carbon column

As the porous-medium ages, the slope of the measured $C(x)$ curve in the “upstream” sections decline, while the slope of the measured $C(x)$ curve in the adjacent downstream sections increase. The “clean” porous-media-column behavior which has been reported earlier (Chatterjee and Shajahan (2010)). This can be attributed to the existence of dual-deposition rates (Tufenkji and Elimelech (2005)). It can also arise from the formation of small colloidal aggregates under the experimental conditions used in this work, as has been shown in Chatterjee and Gupta (2009). It is possible that the 2 deposition rates observed in the clean bed data, arise due to 2 distinct mechanisms of deposition, one operative at the uppermost layers and the other inside the media, such as sieving (Bradford *et al.* (2003)). However, the migration of the regions of maximum slopes with age needs to be explained. It has been suggested (Grolimund *et al.* (2001)), that conditions leading to coagulation of colloids are similar to conditions which lead to significant colloidal deposition, during flow through saturated-porous-media, which was the basis of selection the above electrolytes and their levels for this experimental study. The levels of NaCl and CaCl₂ selected for the experiments are approximately in agreement with the Schulz-Hardy rule with suggests that the critical coagulation concentration for a divalent counter-ion (Ca²⁺) would be lower by a factor of 64 (2^6), than the critical coagulation concentration of the mono-valent counter-ion (Na⁺). The experimental data reported in this paper demonstrates that the above is observed across very different types of media, namely sand and activated carbon.

The overall population displays a high deposition-rate as long as the high-depositing colloids are present in the population. The lower deposition-rate appears when the fast-depositing colloid fraction becomes negligible, for both types of media and electrolyte concentrations. With age, increase in $S(x)$ causes the deposition-loss due to blocking or detachment to become significant. Hence the fast-depositing colloids and colloidal aggregates cannot deposit in the “upstream” section and penetrate further into the media. During this “transient stage” they deposit in the sections where the solid-phase deposit density has not reached a level, significant enough to contribute to deposition-loss. However during this “transient stage” also, the fast-depositing

population depletes below the level of the slow-depositing population within the column. Hence the lower slope of the measured $C(x)$ curve appears, in Figs. 1 to 3, after the fast-depositing population-segment disappears.

The above is evident from the calculated curves for $C_1(x)$ and $C_2(x)$ shown in Fig. 7, obtained using the 2 different sets of parameters, reported in column 1 and column 3 of Table 2. Once again we observe that the above is true across the different media types studied in this work.

Another interesting observation is the near-log-linear nature of the $S(x)$ curve obtained from the sand and activated carbon columns at the end of the experiments. It has been reported that $\log S(x)$ versus x shows a deviation from linearity for systems which show dual deposition-rates (Tufenkji and Elimelech (2005a)). Fig. 8 shows the calculated $S_1(x)$ and $S_2(x)$ after different durations for different conditions. The day 1 (Fig. 8(a)) and day 4 (Fig. 8(b)) deposit density curves show deviation of $S(x)$ from log-linearity. With age the upstream sections of the porous-medium saturates with deposits, which causes the deviation of $S(x)$ from log-linearity to become subdued as seen in Fig. 8(a): Day 5, and Fig. 8(b): Day 20. This suggests that porous media will tend to get uniformly utilized with age in depth filters, till flow rates drop to unacceptable levels.

Fig. 9 shows the calculated porosity variation with distance as the porous-medium ages. It can be observed that the porosity decline starts from the upstream section which gradually penetrates into the column. It can be seen that all extended-time data from the experimental systems studied in this paper, can be explained without using time-dependent deposition-rates. This is in contrast to several earlier models which have used time or deposit-density dependent deposition-rate, (Gitis *et al.* 2010, Mackie and Zhao (1999)), for different experimental systems.

The above discussion shows that the dual deposition-rate based model for colloid filtration with provision for the “deposition-loss” rate, can explain the observed behavior for the different experimental systems discussed in this paper. However the experimental data shows that the activated carbon based column is much more effective in retaining colloids as compared to the sand column. The highest measured value for the solid phase deposit density for the activated carbon column was 353 mg of colloids/gm of media. The peak value for $S(x)$ for the sand column under the same conditions was 50 mg/gm. This shows that the activated carbon has almost an order of magnitude higher capacity for retaining the colloids used in this work, under similar and favorable conditions, compared to sand. Interestingly the peak $S(x)$ value obtained with the sand media using 200 mM NaCl was 35.4 mg/gm. This suggests that with sand as the media, 3 mM CaCl_2 provides a more favorable condition for colloid deposition as compared to 200 mM NaCl. Hence even when the electrolyte concentration was chosen in excess of the Shultz-Hardy rule, Ca^{2+} shows a disproportionate ability to cause deposition of colloids onto media. The causes of this disproportionate contribution of Ca^{2+} for causing colloid deposition can be explored further.

Comparing the parameter values shown in column 2 and column 3 of Table 2, we observe that the large differences observed between activated carbon and sand, can be explained by lower values of the deposition-loss-rates for activated carbon. The parameter values in table clearly show that the fraction of fast-depositing colloids remains the same in the two experiments with 3 mM CaCl_2 as does the “deposition-rate”. “Deposition-loss-rate” quantifies the loss of deposits from the media surface, which implies that Activated Carbon does not allow deposited colloids to escape. It may alternately be due to the presence of many more sites for deposition in activated carbon, which would delay the onset of “blocking” keeping “blocking-rate” low. Low values of “blocking-rate” also lead to low values of “deposition-loss-rate”. Combination of both or either of the above may be causing the higher solid-phase deposit densities on activated carbon when compared to sand.

6. Conclusions

Based on the experiments and model reported above, we conclude the following:

1. The dual deposition and detachment rate based transient model can be used to predict lifetime data across different types of media for colloid filtration. The above does not require the use of time-dependent or media-state dependent deposition rates.

2. The $S(x)$ data demonstrates the significantly higher capacity of activated carbon to bind the colloids used in this study compared to sand, under these experimental conditions.

3. The parameter values shown in Table 2, give a possible new insight, which can explain the vastly superior performance of activated carbon as compared to sand, under comparable conditions.

4. The parameters in Table 2 suggest that while the deposition rates for the 2 media are same, the difference in performance, is probably due to the difference in the deposition-loss rates for activated carbon and sand.

5. The model suggests that the colloids, once deposited, are much less likely to detach from activated carbon. The low deposition-loss rate could be due to many more sites for deposition, which delays the onset of “blocking” on activated carbon. This makes activated carbon the preferred media for colloid filtration.

References

- Ahmadi, H., Namin, M.M. and Kilanehei, F. (2016), “Development a numerical model of flow and contaminant transport in layered soils”, *Adv. Environ. Res.*, **5**(4), 263-282.
- Bai, R. and Tien, C. (1997), “Particle detachment in deep bed filtration”, *J. Coll. Interf. Sci.*, **186**(2), 307-317.
- Bergendahl, J. and Grasso, D. (2000), “Prediction of Colloid detachment in a model porous media: Hydrodynamics”, *Chem. Eng. Sci.*, **55**(9), 1523-1532.
- Bradford, S.A. and Bettahar, M. (2006), “Concentration dependent transport of colloids in saturated-porous-media”, *J. Contam. Hydrol.*, **82**(1), 99-117.
- Bradford, S.A., Simunek, J., Bettahar, M., Tadassa, Y.F., Th Van Genuchten, M. and Yates, S.R. (2005), “Straining of colloids at textural interfaces”, *Wat. Res. Res.*, **41**(10), W10404.
- Bradford, S.A., Simunek, J., Bettahar, M., Th Van Genuchten, M. and Yates, S.R. (2003), “Modeling colloid attachment, straining and exclusion in saturated-porous-media”, *Environ. Sci. Technol.*, **37**(10), 2242-2250.
- Bradford, S.A., Torkzaban, S. and Walker, S.L. (2007), “Coupling of physical and chemical mechanisms of colloid straining in saturated-porous-media”, *Wat. Res.*, **41**(13), 3012-3024.
- Brown, D.G. and Abramson, A. (2006), “Collision efficiency distribution of a bacterial suspension flowing through porous media and implications for field scale transport”, *Wat. Res.*, **40**(8), 1591-1598.
- Chatterjee, J. and Gupta, S.K. (2014), *Particulate Filter*, EP 2161067 B1.
- Chatterjee, J. and Gupta, S.K. (2009), “An agglomeration-based model for colloid filtration”, *Environ. Sci. Technol.*, **43**(10), 3694-3699.
- Chatterjee, J., Pratap, S. and Shajahan, A. (2011), “Dual-deposition rates in colloid filtration caused by coupled heterogeneities in a colloidal population”, *J. Coll. Interf. Sci.*, **356**(1), 362-368.
- Chatterjee, J., Shajahan, A. and Gupta, S.K. (2010), “Estimation of colloidal deposition from heterogeneous populations”, *Wat. Res.*, **44**(11), 3365-3374.
- Darby, J.L. and Lawler, D.F. (1992), “Filtration of heterogeneous suspensions: Modeling of particle removal and head loss”, *Wat. Res.*, **26**(6), 711-726.

- Foppen, W.J., Herwerden, M. and Schijven, J. (2007), "Transport of escherichia coli in saturated-porous-media: Dual mode deposition and intra-population heterogeneity", *Wat. Res.*, **41**(8), 1743-1753.
- Gitis, V., Rubenstein, I., Livshits, M. and Ziskind, G. (2010), "Deep-bed filtration model with multistage deposition kinetics", *Chem. Eng. J.*, **163**(1), 78-85.
- Grolimund, D., Elimelech, M. and Borkovec, M. (2001), "Aggregation and deposition of mobile colloidal particles in natural porous media", *Coll. Surf. A.*, **191**(1), 179-188.
- Hamid, S. and Lee, W. (2016), "Reduction of nitrate in groundwater by hematite supported bimetallic catalyst", *Adv. Environ. Res.*, **5**(1), 51-59.
- Kalpakh, Y. (2015), "Removal of Cu (II) from aqueous solutions using magnetite: A kinetic, equilibrium study", *Adv. Environ. Res.*, **4**(2), 119-133.
- Li, X., Scheibe, T.D. and Johnson, W.P. (2004), "Apparent decreases in colloid deposition-rate coefficients with distance of transport under unfavorable deposition conditions: A general phenomena", *Environ. Sci. Technol.*, **38**(2), 5616-5625.
- Mackie, R.I. and Zhao, Q. (1999), "A framework for modeling removal in the filtration of poly-disperse suspensions", *Wat. Res.*, **33**(3), 794-806.
- Mohammed, K.R., Ahsan, A., Imteaz, M., El-Sergany, M.M., Nik Daud, N.N., Mohamed, T.A. and Ibrahim, B.A. (2015), "Performance of GACC and GACP to treat institutional wastewater: A sustainable technique", *Membr. Wat. Treat.*, **6**(4), 339-349.
- Rajagopalan, R. and Tien, C. (1977), "Single collector analysis of collection mechanisms in water filtration", *Can. J. Chem. Eng.*, **55**(3), 246.
- Rouabeh, I. and Amrani, M. (2012), "Equilibrium modeling for adsorption of NO₃⁻ from aqueous solution on activated carbon produced from pomegranate peel", *Adv. Environ. Res.*, **1**(2), 143-151.
- Satavalekar, R.S. and Sawant, V.A. (2014), "Numerical modelling of contaminant transport using FEM and mesh-free method", *Adv. Environ. Res.*, **3**(2), 117-129.
- Tien, C. and Ramarao, B.V. (2007), *Granular Filtration of Aerosols and Hydrosols*, Elsevier, New York, U.S.A.
- Tobiason, J.E. and Vigneswaran, B. (1994), "Evaluation of a modified model for deep bed filtration", *Wat. Res.*, **28**(2), 335-342.
- Tong, M. and Johnson, W.P. (2007), "Colloid population heterogeneity drives hyper exponential deviation from classic filtration theory", *Environ. Sci. Technol.*, **41**(2), 493-499.
- Tong, M., Camesano, T.A. and Johnson, W.P. (2005), "Spatial variation in deposition-rate coefficients of an adhesion-deficient bacterial strain in quartz sand", *Environ. Sci. Technol.*, **39**(10), 3679-3687.
- Tufenkji, N. (2007), "Modeling microbial transport in porous media: Traditional approaches and recent developments", *Adv. Wat. Res.*, **30**(6), 1455-1469.
- Tufenkji, N. and Elimelech, M. (2004), "Deviation from the classical colloid filtration theory in the presence of repulsive DLVO interactions", *Langmuir*, **20**(25), 10818-10828.
- Tufenkji, N. and Elimelech, M. (2005a), "Breakdown of colloid filtration theory: Role of the secondary energy minimum and surface charge heterogeneities", *Langmuir*, **21**(3), 841-852.
- Tufenkji, N. and Elimelech, M. (2005b), "Spatial distribution of cryptosporidium oocysts in porous media: Evidence of dual mode deposition", *Environ. Sci. Technol.*, **39**(10), 3620-3629.
- Tufenkji, N., Redman, J.A. and Elimelech, M. (2003), "Interpreting deposition patterns of microbial particles in laboratory scale experiments", *Environ. Sci. Technol.*, **37**(3), 616-623.
- Vigneswaran, S. and Tulachan, R.K. (1998), "Mathematical modeling of transient behavior of deep bed filtration", *Wat. Res.*, **22**(9), 1093-1100.